A Novel Fusion-Based Feature Extraction with an Enhanced Segmentation Method to Improve Breast Cancer Analysis Using Thermogram Imagery

Preethi Veerlapalli
Department of Computer Science and Engineering, Koneru Lakshmaiah Education Foundation, Hyderabad-500075, Telangana, India
preethireddyveerlapalli@gmail.com (corresponding author)

Sushama Rani Dutta
Department of Computer Science and Engineering, Koneru Lakshmaiah Education Foundation, Hyderabad-500075, Telangana, India
sushamarani.dutta@klh.edu.in

Received: 2 August 2025 | Revised: 20 August 2025, 9 September 2025, and 13 September 2025 | Accepted: 15 September 2025

 DOI: https://doi.org/10.48084/etasr.13795

ABSTRACT

Breast Cancer (BC) is a common illness that has received considerable attention in the last few years. Early recognition of this disease is crucial to improving the chances of survival. Thermography is an effective screening tool that can assist in detecting BC by identifying body parts with abnormal temperature variations. For effective BC detection using thermography, it is crucial to identify the Region Of Interest (ROI) in the thermograms before diagnosis. Deep Learning (DL) models currently enable the development of systems for detecting abnormalities from thermogram images. In this study, a Leveraging Antlion Optimization and Fusion Feature for an Enhanced Segmentation Method to Improve Breast Cancer Analysis (LALOFF-SMIBCA) is proposed. This study aims to develop an automatic segmentation model for BC detection using thermogram images, thereby enhancing diagnostic accuracy and efficiency. Initially, the image pre-processing utilizes the Adaptive Bilateral Filtering (ABF) model to remove unwanted noise and enhance image quality. Furthermore, the improved DeepLabv3+ model is employed for segmentation. Moreover, a fusion of the ResNet101, ContextNet, and MobileNetV2 models is implemented for feature extraction. Additionally, a Variational Autoencoder (VAE) is utilized for BC classification. Finally, the parameter tuning process is performed using the utilization optimization method. Experiments with the LALOFF-SMIBCA approach are conducted on the BC diagnosis dataset. The comparison analysis of the LALOFF-SMIBCA approach demonstrated a superior accuracy of 98.54% compared to existing models.

Keywords-breast cancer analysis; segmentation method; antlion optimisation; thermogram imagery; fusion feature extraction

I. INTRODUCTION

BC remains a prevalent type of invasive cancer among women globally. Based on a survey, around 627,000 women have died due to BC, and these numbers are rising worldwide [1]. Initial detection is vital to improve patient outcomes since it enables appropriate intervention and treatment strategies [2]. Currently, numerous imaging modalities exist to diagnose such diseases [3]. Thermography employs a heat-sensing camera to detect temperature differences on the breast surface, as malignant tumors often appear warmer due to increased blood flow and cell activity [4]. Unlike mammography, it is non-invasive and does not require breast compression [5].

During the segmentation process, breast regions are extracted and separated from other body parts in a thermogram [6]. Therefore, segmentation identifies the ROI in the output image. For ROI extraction, automated and manual methods are employed [7]. Manual segmentation is often employed to mitigate segmentation errors that may arise from automated methods [8]. Feature extraction is performed after the breast region is segmented. Currently, Computer-Aided Detection (CAD) shows some development in this domain [9], whereas advanced ML and DL models have confirmed the possibility for the detection and segmentation task [10].

Authors in [11] utilized a multi-resolution ViT-enabled structure with ensemble decision-making. Authors in [12] proposed an automatic CAD scheme. They also employed Otsu's multilevel thresholding paradigm for detection and segmentation. Authors in [13] presented BreastCNet, a CNN with an optimizer and a multi-task learning approach. Authors in [14] proposed a method for transforming ultrasound images into a 3D model using the Point-E system. Moreover, a feature pattern study was used to define the features. Authors in [15] introduced a new CNN-based multi-class tissue segmentation. Authors in [16] presented a UNet-like DL model named DRD-UNet that includes a new processing block termed a Dilation, Residual, and Dense (DRD) block within the UNet architecture. DRD-UNet is used for the semantic segmentation of histological images. Authors in [17] presented an ROI identification model for WSI and applied it to Human Epidermal growth factor Receptor 2 (HER2) grading in BC patients. Authors in [18] developed a framework to identify and delineate cancer regions in mammographic and Breast Ultrasound (BUS) images. Authors in [19] proposed a method incorporating fuzzy fusion-based segmentation (including Rényi Entropy, Level Set, and DeepLabv3+), Enhanced Snake Optimization (ESO) for feature selection, and ensemble AdaBoost for classification. Authors in [20] presented a model by integrating radiomic features with DL features using Recursive Feature Elimination (RFE) and an ensemble of ML classifiers for classification. Authors in [21] proposed a method using a custom CNN integrated with Histogram of Oriented Gradients (HOG) features. Authors in [22] introduced a novel Stack Visual Representation Deep Network (StackVRDNet) technique. The model also utilized VGG16, ResNet, and DenseNet, with Rock Hyraxes' Dandelion Algorithm Optimization (RHDAO) for optimization. Several models depend on single-modality data or lack extensive validation on diverse datasets. The research gap is in integrating multi-modal features with robust optimization techniques to enhance generalizability and accuracy.

This study proposes the LALOFF-SMIBCA method, and the major contributions of the method are listed below.

- The ABF model is used during pre-processing to improve thermal images by effectively eliminating noise while preserving critical edge details, thereby preserving diagnostic features and enhancing downstream segmentation and accuracy.
- The improved DeepLabv3+ model is employed to build a robust segmentation process that accurately delineates breast regions from thermal imagery, enabling precise localization of potential abnormalities and improving the overall diagnostic framework.
- A fusion-based feature extraction approach is used to capture multi-scale, contextual, and deep semantic features from images, incorporated with a VAE model for BC classification and an ALO method for parameter tuning to improve accuracy and generalization.
- The novelty is in the integration of ABF for image enhancement, multi-network feature fusion, DeepLabv3+ for precise segmentation, VAE for classification, and ALO for tuning, creating a comprehensive and accurate framework for BC detection using thermal images.

II. METHODOLOGICAL FRAMEWORK

In this manuscript, the LALOFF-SMIBCA technique is proposed. It comprises pre-processing, segmentation, BC classification, and optimization. Figure 1 illustrates the complete procedure of the LALOFF-SMIBCA model.

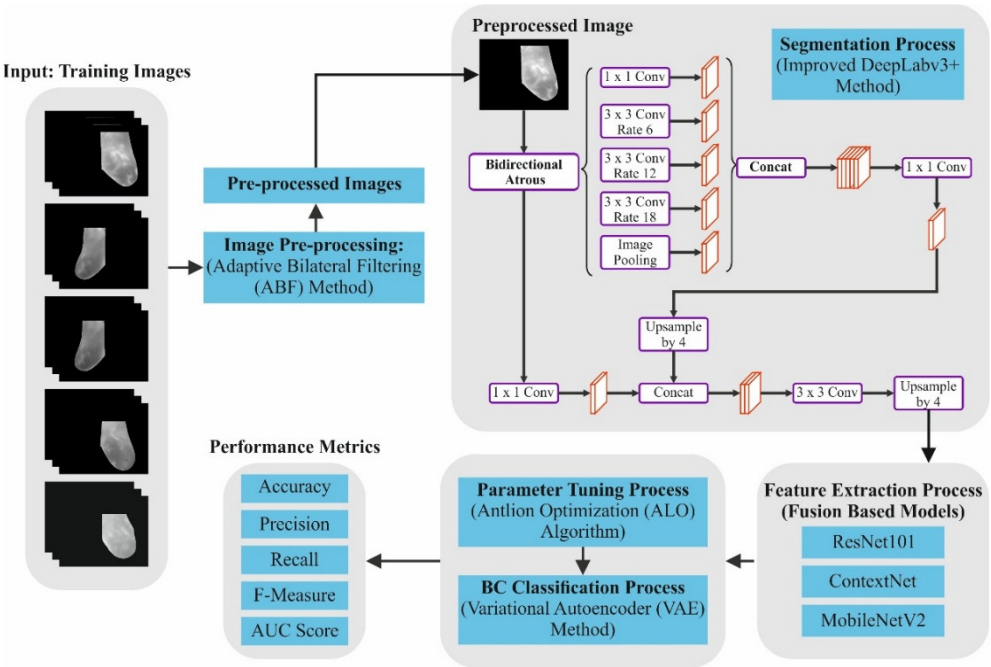

Fig. 1. Entire procedure of the LALOFF-SMIBCA model.

A. ABF-Based Pre-Processing Technique

ABF is an effective image processing method, which is employed to improve thermogram images for automated segmentation in BC diagnosis [23]. This method is chosen for its capability to mitigate noise while preserving critical edge details, a feature essential for precise detection. This model also adapts its parameters locally, ensuring sharper boundary preservation around anomalies. This makes it more effective than conventional smoothing models in highlighting subtle thermal discrepancies for diagnosis. It maintains edge details while efficiently reducing noise, which is vital in thermal images where subtle temperature variations indicate potential anomalies. Unlike typical smoothing filters, the ABF alters its parameters depending on local image features, which ensures sharper boundary preservation around cancerous regions. This filtering stage enhances the precision of thermal patterns, which makes it simpler to isolate precisely. In BC recognition, these methods aim to better contrast between abnormal and normal tissues.

B. Segmentation Using the DeepLabv3+ Method

Next, the improved DeepLabv3+ method is used for segmentation [24]. This method is chosen for its efficiency in capturing multi-scale contextual data using Atrous Spatial Pyramid Pooling (ASPP). The accuracy of segmentation on intrinsic thermal images is improved, and the encoder-decoder architecture effectively refines object boundaries, making it appropriate for precise breast region delineation. The technique also offers superior performance with efficient computation. Its effectiveness relies on the ASPP component. A DeepLab-v3-based decoder framework that improves segmentation edge precision by integrating original and high-level features is utilized. It employs dilated convolutions to expand the receptive field without losing spatial resolution, enabling better contextual comprehension and improved segmentation accuracy:

$$K = k + (k-1)(r-1) \quad (1)$$

where k represents the original Conv kernel size, and r signifies the dilation rate.

C. Fusion of Feature Extraction Process

Moreover, a fusion of ResNet101, ContextNet, and MobileNetV2 models is utilized for feature extraction. This ensemble is chosen for its complementary strengths in extracting deep features, capturing context, and efficient (lightweight) processing, respectively. This integration improves multi-scale and contextual feature representation, thereby enhancing accuracy and robustness compared to utilizing a single model.

1) ResNet101 Technique

ResNet-101 is a deep residual network comprised of 101 layers with an identity shortcut connection that effectively mitigates the degradation problem in deep networks [25]. Its framework ensures stable training and captures valuable multi-scale semantic features from complex images. ResNet101 serves as the backbone, extracting deep features via a 7×7 Conv, downsampling, and bottleneck residual blocks. Global average pooling reduces features before classification, with batch normalization enhancing training stability and speed.

2) ContextNet Model

The basic framework of ContextNet is a sequential stack of context blocks [26]. Conv layers with varied receptive fields are combined using dual parallel kernels: 1x1 point-wise Conv for channel-wise integration and 3x3 Conv for local spatial features. Given input feature map $F \in X^{W\times H\times C}$, WxH is the spatial size, and C is the channel count

$$\begin{cases} Y_1 = \frac{1}{4}\sum_{u=0}^{1}\sum_{v=0}^{1}\left(\sum_{d=1}^{c} X\,(2i+u, 2j+v, d)\cdot W_1(d,k) + b(k)\right) \\ Y_2 = \sum_{u=-1}^{1}\sum_{v=-1}^{1}\sum_{d=1}^{c} X\left(i+u^{'}, j+v^{'}, d\right)\cdot W_2(d, u+1, v+1, k) + b(k) \\ Y_3 = \sum_{u=-1}^{1}\sum_{v=-1}^{1}\sum_{d=1}^{c} X\left(i+2u^{'}, j+2v^{'}, d\right)\cdot W_3(d, u+1, v+1, k) + b(k) \end{cases} \quad (2)$$

$Y1$, $Y2$, and $Y3$ depict the feature maps from point-wise Conv, 3×3 dilated Conv, and 3×3 Conv, respectively. A point-wise convolution refines channels for compact, context-rich features:

$$Y = Conv_{1\times1}\left(Concat(Y_1 + Y_2 + Y_3)\right) \quad (3)$$

3) MobileNetV2 Method

MobileNet-V2 forms a parallel path using stacked Inverted Residual Blocks (IRB) and depth-wise separable convolutions to efficiently capture multi-scale features in a lightweight structure [27]. The output feature map from MobileNetV2 is then input to the ASPP component. Assuming its input feature map is $\in Z^{W\times H\times C}$, the output feature map from the ASPP unit is A:

$$\begin{cases} A_1 = \sum_{d=1}^{c} Z(i,j,d)\cdot W_1'(d,k) + b(k) \\ A_2 = \sum_{u=-1}^{1}\sum_{v=-1}^{1}\sum_{d=1}^{c} Z\,(i+u', j+v', d)\cdot W_2'(d, u+1, v+1, k) + b(k) \\ A_3 = \sum_{u=-1}^{1}\sum_{v=-1}^{1}\sum_{d=1}^{c} Z\,(i+4u', j+4v', d)\cdot W_3'(d, u+1, v+1, k) + b(k) \\ A_4 = \sum_{u=-1}^{1}\sum_{v=-1}^{1}\sum_{d=1}^{c} Z\,(i+8u', j+8v', d)\cdot W_4'(d, u+1, v+1, k) + b(k) \end{cases} \quad (4)$$

Then, ASPP utilizes a feature concatenation approach for integrating the output in the dimension of the channel, while maintaining the richer contextual and multi-scale feature data:

$$A = Conv_{1\times1}(Concat(A_1 + A_2 + A_3 + A_4)) \quad (5)$$

D. VAE-Based BC Classification Procedure

VAE is a generative method that comprises an encoder and decoder, equivalent to AE [28]. This method is chosen for its capability in learning robust latent representations by modelling data distributions, which improves accuracy. The model also effectively handles intrinsic feature spaces and mitigates overfitting through regularization, making it appropriate for BC classification from fused deep features. The encoder is represented by $q_\phi(c|b)$, mapping data y to the hidden space, and the decoder $p_\theta(b|c)$ endeavours to rebuild the data y from these hidden variables. The objective function of VAE is typically formulated as maximizing the Evidence Lower Bound (ELBO):

$$\arg\min_{\phi,\theta}\{\mathbb{E}_{q_\phi(c|b)}[logp_\theta(b|c)] - D_{KL}(q_\phi(c|b)||p(c))\} \quad (6)$$

The CVAE extends VAEs into a conditional generative model comprising hidden, input, and output variables: c, a, and b. Either encoding or decoding of CVAE methodologies is conditioned on the input variable a, depicted as $q_\phi(c|b,a)$ and $p_\theta(b|c,a)$, correspondingly:

$$\arg\max_{\phi,\theta}\{\mathbb{E}_{q_\phi(c|b)}[\log p_\theta(b|c)] - D_{KL}(q_\phi(c|b)||p(c))\} \quad (7)$$

E. Parameter Tuning Using the ALO Approach

Finally, parameter tuning is performed using the ALO approach [29]. This approach is chosen for its effective global search capability and fast convergence. It also effectively balances exploration and exploitation, resulting in an enhanced model performance and reducing the risk of becoming trapped in local minima during parameter tuning. Antlions show a complex hunting tactic that acts as the inspiration for the ALO, a novel metaheuristic algorithm based on the intelligence of swarms. The initial populations for both antlions and ants are initialized at random, as delineated in (8):

$$x = \text{rand} \times (UPB - LOB) + LOB \quad (8)$$

Equation (8) depicts the upper and lower limits as UPB and LOB, respectively. The random walking procedure for all ants in the iterations is shown in (9):

$$X(t) = [0, Csum(2r(t_1) - 1), \ldots, Csum(2r(t_T) - 1)] \quad (9)$$

To ensure the ant stays within the search boundaries, the procedure is normalized using predefined lower and upper limits:

$$X_i^t = \frac{(X_i^t - a_i)^*(b_i - c_i^t)}{(a_i^t - a_i)} + c_i \quad (10)$$

where b_i and a_i depict the random walk's maximal and minimal values for the ith variable; and, d_i^t and c_i^t specify the maximal and minimal values of the ith variable at the tth iteration:

$$\begin{aligned} c_i &= antlion + c_i \\ d_i &= antlion + d_i \end{aligned} \quad (11)$$

The initial antlion, selected using RWS, is considered the winner, whereas the best-performing antlion (elite antlion) is identified based on fitness evaluation:

$$Ant_i^t = \frac{R_A^t + R_E^t}{2} \quad (12)$$

Ant_i^t represents the location of the ith and tth iterations. R_A^t characterizes the random walks near the particular antlion in the tth iteration; however, R_E^t signifies the random walks near the best antlion from these iterations:

$$\begin{aligned} c^t &= c^t / I \\ d^t &= d^t / I \end{aligned} \quad (13)$$

The ALO model initiates an FF to achieve improved classification performance. The classification rate of error reduction was designated as FF:

$$\begin{aligned} fitness(x_i) &= ClassifierErrorRate(x_i) \\ &= \frac{\text{no.of misclassified samples}}{\text{Total no.of samples}} \times 100 \end{aligned} \quad (14)$$

III. PERFORMANCE ASSESSMENT

The performance of the LALOFF-SMIBCA is evaluated on the BC diagnosis dataset [30]. The method runs on Python 3.6.5 with an i5-8600k CPU, 4GB GPU, 16GB RAM, 250GB SSD, and 1TB HDD, using a 0.01 learning rate, ReLU, 50 epochs, 0.5 dropout, and batch size 5. The dataset has 1280 images and has two kinds of tumors, namely benign and malignant tumors, each containing 640 images. Figure 2 represents the sample image. Table I depicts the BC detection of the LALOFF-SMIBCA model at 80:20 of TRPHE/TSPHE.

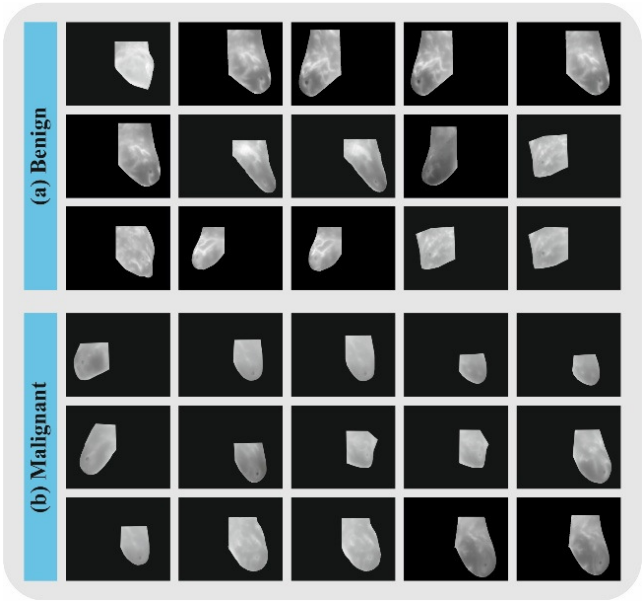

Fig. 2. (a) Malignant images and (b) benign images.

TABLE I. BC DETECTION OF LALOFF-SMIBCA AT 80:20 OF TRPHE/TSPHE

Class Labels	$Accu_y$	$Prec_n$	$Reca_l$	$F_{Measure}$	AUC_{score}
TRPHE (80%)					
Benign	98.05	99.02	98.05	98.53	98.54
Malignant	99.02	98.06	99.02	98.54	98.54
Average	98.54	98.54	98.54	98.54	98.54
TSPHE (20%)					
Benign	96.85	100.00	96.85	98.40	98.43
Malignant	100.00	96.99	100.00	98.47	98.43
Average	98.43	98.50	98.43	98.44	98.43

Table II presents a comparison of the LALOFF-SMIBCA method with recent models [31-33]. The output showed that the ResNet50, VGG16, Swin-B, SVM, Naïve Bayes (NB), ANN, InceptionNetV3, and EfficientNet-B0 models demonstrated the worst performance. Whereas, the LALOFF-SMIBCA model attains maximum $Accu_y$, $Prec_n$, $Reca_l$ and $F_{Measure}$ of 98.54%, 98.54%, 98.54%, and 98.54%, respectively.

TABLE II. COMPARATIVE ANALYSIS OF LALOFF-SMIBCA MODEL WITH RECENT METHODS [31-33]

Technique	$Accu_y$	$Prec_n$	$Reca_l$	$F_{Measure}$
ResNet50	88.60	85.10	89.25	89.00
VGG16	91.90	81.10	81.40	81.30
Swin-B	88.60	85.30	87.10	86.50
SVM	97.33	91.85	95.73	97.28
CNN Base Model	75.00	74.00	75.00	75.00
MobileNetV3	89.00	90.00	89.00	89.00
InceptionNetV3	95.00	95.00	95.00	95.00
EfficientNet-B0	85.00	86.00	86.00	86.00
LALOFF-SMIBCA	98.54	98.54	98.54	98.54

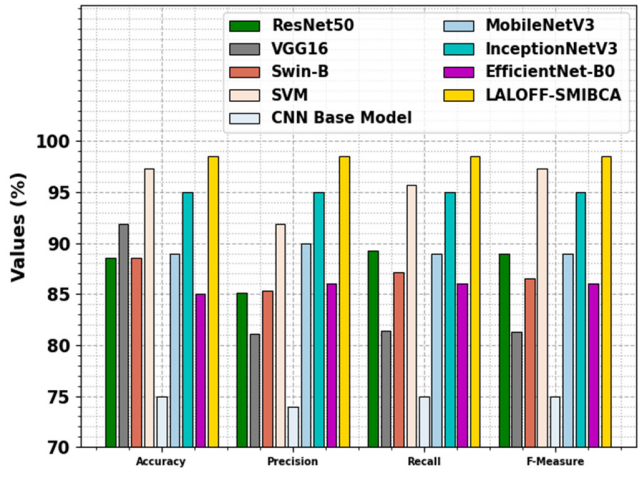

Fig. 3. Comparative results of the proposed model vs. existing models.

Table III demonstrates the ablation study of the LALOFF-SMIBCA method. The obtained values demonstrated the results of the LALOFF-SMIBCA method with single feature extractor, with fusion process, classifier without parameter optimization, and classifier with parameter optimization. The experimental values highlighted that the single feature extractor models exhibit reduced classification results. At the same time, the fusion model achieves improved results over other feature extractors. Besides, the VAE classifier leads to moderately improved performance and the application of ALO helps in accomplishing even better performance. However, the proposed model exhibits improved results over the other models.

TABLE III. RESULT ANALYSIS OF THE ABLATION STUDY OF THE LALOFF-SMIBCA METHODOLOGY

Model	$Accu_y$	$Prec_n$	$Reca_l$	$F_{Measure}$
ResNet101	94.88	95.35	94.87	95.30
ContextNet	95.54	95.90	95.65	95.98
MobileNetV2	96.29	96.60	96.43	96.50
Fusion model	96.89	96.87	96.78	96.98
VAE	97.09	97.25	97.21	97.12
ALO-VAE	97.86	97.79	97.94	97.87
LALOFF-SMIBCA	98.54	98.54	98.54	98.54

IV. CONCLUSION

The LALOFF-SMIBCA model is proposed. Initially, the ABF approach was utilized. Furthermore, the improved DeepLabv3+, fusion-based feature extraction models, VAE, and ALO are used for segmentation, extraction, classification, and parameter tuning. Experiments on the BC diagnosis dataset demonstrated a superior accuracy of 98.54% compared to existing models. The limitations include the use of a relatively limited dataset and the lack of real-time testing. Future work may concentrate on evaluating the model on larger, more diverse datasets, exploring its feasibility for real-time clinical use, and integrating multi-modal imaging such as mammography and ultrasound for improved diagnostic performance. Moreover, future studies may focus on integrating adaptive learning methods to dynamically adjust parameters for improved performance across varying datasets and conditions.

APPENDIX

The data that support the findings of this study are openly available in the Kaggle dataset https://www.kaggle.com/datasets/faysalmiah1721758/breast-cancer-diagnosis [30].

REFERENCES

[1] D. Sánchez-Ruiz, I. Olmos-Pineda, and J. A. Olvera-López, "Automatic region of interest segmentation for breast thermogram image classification," *Pattern Recognition Letters*, vol. 135, pp. 72–81, July 2020, https://doi.org/10.1016/j.patrec.2020.03.025.

[2] N. Venkatachalam, L. Shanmugam, G. C. Heltin, G. Govindarajan, and P. Sasipriya, "Enhanced Segmentation of Inflamed ROI to Improve the Accuracy of Identifying Benign and Malignant Cases in Breast Thermogram," *Journal of Oncology*, vol. 2021, no. 1, 2021, Art. no. 5566853, https://doi.org/10.1155/2021/5566853.

[3] O. I. Ramadan *et al.*, "Enhancing Breast Cancer Classification based on BPSO Feature Selection and Machine Learning Techniques," *Engineering, Technology & Applied Science Research*, vol. 15, no. 3, pp. 23907–23916, June 2025, https://doi.org/10.48084/etasr.10900.

[4] A. S. Hakim and R. N. Awale, "Extraction of hottest blood vessels from breast thermograms using state-of-the-art image segmentation methods," *Quantitative InfraRed Thermography Journal*, vol. 19, no. 5, pp. 347–365, Oct. 2022, https://doi.org/10.1080/17686733.2021.1974209.

[5] T. Trongtirakul, S. Agaian, A. Oulefki, T. Trongtirakul, S. Agaian, and A. Oulefki, "Automated tumor segmentation in thermographic breast

images," *Mathematical Biosciences and Engineering*, vol. 20, no. 9, pp. 16786–16806, 2023, https://doi.org/10.3934/mbe.2023748.

[6] K. F. F. C. da Queiroz, J. R. A. de Queiroz Júnior, H. Dourado, and R. de C. F. de Lima, "Automatic segmentation of region of interest for breast thermographic image classification," *Research on Biomedical Engineering*, vol. 39, no. 1, pp. 199–208, Mar. 2023, https://doi.org/10.1007/s42600-023-00265-z.

[7] S. M. Shaaban, M. Nawaz, Y. Said, and M. Barr, "An Efficient Breast Cancer Segmentation System based on Deep Learning Techniques," *Engineering, Technology & Applied Science Research*, vol. 13, no. 6, pp. 12415–12422, Dec. 2023, https://doi.org/10.48084/etasr.6518.

[8] D. Tsietso, A. Yahya, and R. Samikannu, "A Review on Thermal Imaging-Based Breast Cancer Detection Using Deep Learning," *Mobile Information Systems*, vol. 2022, no. 1, 2022, Art. no. 8952849, https://doi.org/10.1155/2022/8952849.

[9] T.-N. Nguyen, T.-T. Nguyen, T.-H. Nguyen, and B.-V. Ngo, "A Robust Approach for Breast Cancer Classification from DICOM Images," *Engineering, Technology & Applied Science Research*, vol. 15, no. 3, pp. 23499–23505, June 2025, https://doi.org/10.48084/etasr.10931.

[10] S. Kaur, J. D. Kumar, G. Chaudhary, and M. Khari, "Breast Cancer Detection Using Deep Learning and Feature Decision Level Fusion," *Fusion: Practice and Applications*, no. 1, pp. 50–59, Jan. 2022, https://doi.org/10.54216/FPA.080105.

[11] M. Sabry *et al.*, "Enhancing Breast Cancer Diagnosis With Multi-Resolution Vision Transformers and Robust Decision-Making," *IEEE Access*, vol. 13, pp. 89704–89722, 2025, https://doi.org/10.1109/ACCESS.2025.3570840.

[12] T. Andreadis, K. Chouchos, N. Courcoutsakis, I. Seimenis, and D. Koulouriotis, "Development of an Automated CAD System for Lesion Detection in DCE-MRI," *Journal of Imaging Informatics in Medicine*, Feb. 2025, https://doi.org/10.1007/s10278-025-01445-2.

[13] H. Mahichi, V. Ghods, M. K. Sohrabi, and A. Sabbaghi, "BreastCNet: Breast Cancer Detection, Classification, and Localization Convolutional Neural Network With Advanced Optimization Techniques," *IEEE Access*, vol. 13, pp. 87386–87400, 2025, https://doi.org/10.1109/ACCESS.2025.3570364.

[14] S. S. Chowa, S. Azam, S. Montaha, M. R. I. Bhuiyan, and M. Jonkman, "Improving the Automated Diagnosis of Breast Cancer with Mesh Reconstruction of Ultrasound Images Incorporating 3D Mesh Features and a Graph Attention Network," *Journal of Imaging Informatics in Medicine*, vol. 37, no. 3, pp. 1067–1085, June 2024, https://doi.org/10.1007/s10278-024-00983-5.

[15] A. Modi *et al.*, "Multi-Stain Multi-Level Convolutional Network for Multi-Tissue Breast Cancer Image Segmentation." arXiv, June 09, 2024, https://doi.org/10.48550/arXiv.2406.05828.

[16] M. A. Ortega-Ruíz, C. Karabağ, E. Roman-Rangel, and C. C. Reyes-Aldasoro, "DRD-UNet, a UNet-Like Architecture for Multi-Class Breast Cancer Semantic Segmentation," *IEEE Access*, vol. 12, pp. 40412–40424, 2024, https://doi.org/10.1109/ACCESS.2024.3377428.

[17] M. S. Hossain *et al.*, "Region of interest (ROI) selection using vision transformer for automatic analysis using whole slide images," *Scientific Reports*, vol. 13, no. 1, July 2023, Art. no. 11314, https://doi.org/10.1038/s41598-023-38109-6.

[18] M. Ahmadi *et al.*, "Comparative Analysis of Segment Anything Model and U-Net for Breast Tumor Detection in Ultrasound and Mammography Images." arXiv, Feb. 13, 2024, https://doi.org/10.48550/arXiv.2306.12510.

[19] V. Dubey, D. S. Rathore, and D. R. Gedam, "A Novel Fuzzy Fusion-Based Segmentation with Enhanced Feature Selection for Improved Breast Cancer Detection," *Cuestiones de Fisioterapia*, vol. 54, no. 2, pp. 513–532, Jan. 2025.

[20] T. Varshney, K. Verma, A. Kaur, and S. K. Puri, "Hybrid and optimized feature fusion for enhanced breast cancer classification," *Network Modeling Analysis in Health Informatics and Bioinformatics*, vol. 14, no. 1, Aug. 2025, Art. no. 81, https://doi.org/10.1007/s13721-025-00573-7.

[21] A. V. Ikechukwu, S. Bhimshetty, D. R, and M. V. Mala, "Advances in Thermal Imaging: A Convolutional Neural Network Approach for Improved Breast Cancer Diagnosis," in *2024 International Conference on Distributed Computing and Optimization Techniques (ICDCOT)*, Mar. 2024, pp. 1–7, https://doi.org/10.1109/ICDCOT61034.2024.10515323.

[22] A. Y. A. Bani Ahmad, J. A. Alzubi, M. Vasanthan, S. B. Kondaveeti, J. Shreyas, and T. P. Priyanka, "Efficient hybrid heuristic adopted deep learning framework for diagnosing breast cancer using thermography images," *Scientific Reports*, vol. 15, no. 1, Apr. 2025, Art. no. 13605, https://doi.org/10.1038/s41598-025-96827-5.

[23] S. Abdel-Khalek, "Leveraging Quantum Neural Networks with Deep Learning Based Edge Detection Model for Breast Cancer Screening using Digital Mammograms," *Journal of Intelligent Systems and Internet of Things*, no. 2, pp. 68–81, Jan. 2025, https://doi.org/10.54216/JISIoT.160206.

[24] Y. Zhong *et al.*, "Deep Learning-Based Layout Analysis Method for Complex Layout Image Elements," *Applied Sciences*, vol. 15, no. 14, Jan. 2025, Art. no. 7797, https://doi.org/10.3390/app15147797.

[25] T. Ye, M. He, Y. Wang, J. Wang, L. Zhu, and J. Zhang, "An Optimized Intelligent Segmentation Algorithm for Concrete Cracks Based on Transformer," *Electronics*, vol. 14, no. 9, Jan. 2025, Art. no. 1720, https://doi.org/10.3390/electronics14091720.

[26] M. F. Ghobrial, A. M. Gody, and S. T. Muhammad, "Comparative Study on End-to-End Speech Recognition Using Pre-trained Models," *Fayoum University Journal of Engineering*, vol. 8, no. 1, pp. 131–142, Jan. 2025, https://doi.org/10.21608/fuje.2024.312102.1089.

[27] S. Yang *et al.*, "Optimizing foreign fiber segmentation performance with DeepLab V3+ and GAN in industrial IoE environments," *Digital Communications and Networks*, Mar. 2025, https://doi.org/10.1016/j.dcan.2025.03.005.

[28] J. Zhao, Y. Song, and E. Cohen, "Variational Prefix Tuning for diverse and accurate code summarization using pre-trained language models," *Journal of Systems and Software*, vol. 229, Nov. 2025, Art. no. 112493, https://doi.org/10.1016/j.jss.2025.112493.

[29] A. Abdelaziz, A. N. Mahmoud, V. Santos, and M. M. Freire, "Integrating temporal convolutional networks with metaheuristic optimization for accurate software defect prediction," *PLOS ONE*, vol. 20, no. 5, May 2025, Art. no. e0319562, https://doi.org/10.1371/journal.pone.0319562.

[30] "Breast Cancer Diagnosis." https://www.kaggle.com/datasets/faysalmiah1721758/breast-cancer-diagnosis

[31] Y. Mo *et al.*, "HoVer-Trans: Anatomy-Aware HoVer-Transformer for ROI-Free Breast Cancer Diagnosis in Ultrasound Images," *IEEE Transactions on Medical Imaging*, vol. 42, no. 6, pp. 1696–1706, June 2023, https://doi.org/10.1109/TMI.2023.3236011.

[32] U. Naseem *et al.*, "An Automatic Detection of Breast Cancer Diagnosis and Prognosis Based on Machine Learning Using Ensemble of Classifiers," *IEEE Access*, vol. 10, pp. 78242–78252, 2022, https://doi.org/10.1109/ACCESS.2022.3174599.

[33] S. Aziz, K. Munir, A. Raza, M. S. Almutairi, and S. Nawaz, "IVNet: Transfer Learning Based Diagnosis of Breast Cancer Grading Using Histopathological Images of Infected Cells," *IEEE Access*, vol. 11, pp. 127880–127894, 2023, https://doi.org/10.1109/ACCESS.2023.3332541.